Eksplorium *p*-ISSN 0854-1418
Volume 46 No. 1, May 2025: 1367–1375 *e*-ISSN 2503-426X

A New Lattice Hydrodynamic Model for Traffic Flow on Curved Road

Rinku[1], Vivek Kumar Sharma[1*]
[1,1*]Jagannath University, Jaipur, 303901, Rajasthan, India

Article Received: 15 March 2025, Revised: 25 April 2025, Accepted: 28 May 2025

Abstract: Due to topographical features, economic considerations, and driving safety, roads in actual traffic scenarios are often constructed with curves. Therefore, it is important to explore how traffic flow is influenced by curved roads. To analytically examine traffic behavior on such roads, this study introduces an extended lattice hydrodynamic model for curved road conditions. Using linear stability analysis, the conditions for traffic stability are derived. The findings indicate that traffic stability is influenced by factors such as the curvature of road, friction coefficient and turning angle of the road. Furthermore, the Korteweg–de Vries (KdV) equation, and the modified KdV equation are obtained to represent nonlinear density waves in stable, metastable, and unstable traffic regimes, respectively. Numerical simulations are conducted to support the analytical findings. Both theoretical analysis and simulation results demonstrate that traffic flow is significantly affected by the curvature and the curve angle of the road. Additionally, these factors also have an impact on the maximum theoretical traffic flux and vehicle speed.

Keywords: Curvature of the Road, Lattice model, Simulation, Traffic.

INTRODUCTION

The smooth operation of modern society depends on the smooth flow of traffic on road networks, and the traffic flow is crucial to the planning and administration of transportation. Traffic flow has become a critical concern in social problems, with traffic congestion resulting in both disruption and potential safety.

(a) (b)

Figure 1: Visual representation of traffic

Therefore, traffic flow has become a major focus for research. For a more comprehensive understanding of traffic flow, there is a demand for accurate and quantitative models that can forecast all traffic situations based on specific infrastructure. While of the available research has been devoted to understanding traffic behavior on straight road segments. Firstly Nagatani[1], in 1998 originally derived the lattice hydrodynamics model. Additionally, some other mathematical models by Wang[2, 3],Cheng[4], Du[5], Zhang[6], Yu[7], Mohan[8], Gupta[9], Jiang[10], Wanger[11] have been pro-posed. Subsequently, significant research efforts have been dedicated to the examination of the various factors such as backward looking effect, memory effect [12,13].The dynamics of traffic flow around curved road sections present unique challenges and opportunities. Here traffic is moving on a curved road as shown in Fig.

1(a) and Fig. 1(b) provides an explanation of Fig. 1(a). Numerous studies have investigated traffic flow characteristics on curved roads, recognizing the significant influence of road geometry on vehicle dynamics and overall traffic behavior. Notably, researchers such as Zhou[14], Jin[15], Wang [16], Kaur[17],Cao[18], and Wang[19] The later work by Wang[20] further refined the modeling of curved road sections, offering insights into congestion dynamics and system optimization. Collectively, these studies emphasize that a comprehensive understanding of how road curvature influences traffic flow is essential for optimizing highway design, alleviating congestion, and enhancing roadway safety, particularly in modern urban and high-speed transportation networks." "Nagatani introduced a single-lane lattice hydrodynamic model, which provided a fundamental framework for understanding traffic flow in a simplified one-lane scenario. Following this, several researchers extended the lattice hydrodynamic model to account for curved road conditions, adapting the model to better reflect the complexities introduced by length of the curve according to radius of curvature. However, despite these advances, no study has yet reached a conclusive determination of how the road curvature specifically influences the flow of traffic. This gap in the research highlights the need for further exploration of how road curvature, particularly radius of curvature, affects vehicle dynamics, traffic congestion, and overall flow patterns in such settings. This study introduces a novel lattice hydrodynamic model specifically designed to investigate the impact of the road curvature during traffic flow. The lattice hydro- dynamic approach combines elements of both macroscopic and microscopic modeling, allowing for a more detailed examination of traffic dynamics while accounting for the curvature of the road. By incorporating interactions among vehicles and considering the curvature of the road, our model provides a unique framework for studying the complex relationships between vehicle movements and road geometry. Through extensive simulations analysis, the aim of the pro- posed model to elucidate how variations in the road curvature affect traffic flow.

2 PROPOSED MODEL:

Initially, Nagatani[1] developed one lane lattice hydrodynamic model is

$$\partial_t \rho_j + \rho_0(\rho_j v_j - \rho_{j-1} v_{j-1}) = 0 \quad (1)$$

$$\partial_t \rho_j v_j = a\rho_0 V(\rho_{j+1}) - a\rho_j v_j \quad (2)$$

Where "a" symbolize the driver's sensitivity coefficient and ρ_0 stands for the average density. The terms $\rho_j(t)$ and $v_j(t)$specifically indicate the density and velocity at the jth lattice point, respectively. According to Bando et al. [21], the optimal velocity function is specified as

$$V(\rho_{j+1}) = \tanh[(\frac{2}{\rho_0} - \frac{\rho}{\rho_0^2} - \frac{1}{\rho_c}) + \tanh(\frac{1}{\rho_c})] \quad (3)$$

Here Vmax and ρ_c stand for maximum velocity and critical density respectively. Numerous studies have examined both curved highways and straight road segments with a variety of influencing factors. But up until now, road curvature hasn't been taken into account. The curvature R of a curve at a specific point measures the rate at which the curve deviates from a straight line. For a curve y = $\sqrt{A-(x-A)^2}$ where A represent the radius of curvature of the curved road. The curvature R is given by the following formula: R = $\frac{|y''|}{(1+y'^2)^{\frac{3}{2}}}$. The lattice spacing between the site j and j−1 is $l = \int_{x-x_0}^{x} \sqrt{1+y'^2} = \frac{x_0}{sin\theta_j}$. where θ_j represents the radian at jth site of curved road. The modified lattice spacing of the curved road can be used to compute the average headway on curved road in terms of average headway on a straight road ($1/\rho_0$). Therefore, the basic lattice model of Nagatani is modified for

$\partial_t \rho_j + \frac{\rho_0}{sin\theta_j}\left((\rho_j v_j - \rho_{j-1}v_{j-1}\right) = 0$ and $(\rho_j(t+\tau)v_j(t+\tau) = \frac{\rho_0}{sin\theta_j}\mathrm{V}(\rho_{j+1}))$

A LH model that takes into account the curvature of the road was proposed to close this gap and investigate methods of improving driver safety, driver training, and the development of driver-assistance technologies that are more human-limit compatible. The curvature of a road is the reciprocal of the radius of the road's path at a given point. A road with a larger radius of curvature will be less curved (gentler curve), while a road with a smaller radius will be more sharply curved. This formula shows the relationship between the average headway on the straight road and the one on the curved road. Particularly significant on curved roads where safety concerns require slower driving, so velocities should be lower than maximum. A suggested lattice model is explained as follows in order to investigate the importance of road curvature for significant elements influencing driving behavior. A proposed lattice model is explained as follows in order to investigate the significance of road curvature for curved roads:

$$\partial_t \rho_j + \rho_0\left((1+R)(\rho_j v_j - \rho_{j-1}v_{j-1})\right) = 0 \tag{4}$$
$$\partial_t \rho_j v_j = a\rho_0(1+R)(V(\rho_{j+1}) - a\rho_j v_j) \tag{5}$$

Where $q_j = \rho_j v_j$, R is curvature of road during traffic flow and A = 1/R is the radius of the curvature curved road as $R = \frac{|y''|}{\left(1+y'^2\right)^{\frac{3}{2}}}$. Here y′ is the first derivative of the function, representing the slope of the curve and y″ is the second derivative, which gives the rate of change of the slope and, consequently, the curvature. The term $\left(1+y'^2\right)^{\frac{3}{2}}$ accounts for the effect of the curve's steepness on the radius. In curved road scenario, the updated optimized velocity function is

$$V(\rho_{j+1}) = \frac{k\sqrt{\mu g A}}{2}\tanh\left[\frac{2}{\rho_0} - \frac{\rho}{\rho_0^2} - \frac{1}{\rho_c}\right) + \tanh\left(\frac{1}{\rho_c}\right). \tag{6}$$

The maximum linear velocity is denoted as Vmax and determined by $\sqrt{\mu g A}$, where μ stands for the friction coefficient, g represents gravitational force, and k is the controlling parameter for Vmax. In severe curves or turns, the radius of curvature is at its minimum, resulting in the highest curvature. This idea is essential to road design in order to make curves safe for drivers by accounting for variables like vehicle stability and speed. To increase safety and comfort on roads with significant curvature, super elevation and transition curves are frequently used to manage curvature. After removing velocity v_j from Eqs. (4) and (5), model equation obtained as:

$$\left(\rho_j(t+2\tau) - \rho_j(t+2\tau)\right) + \tau\rho_0^2(1+R^2)[\,V\left(\rho_{j+1}(t)\right) - V\left(\rho_j(t)\right)] = 0 \tag{7}$$

3. LINEAR ANALYSIS:

To analyze the linear stability of the proposed model the density of traffic and the optimal velocity under uniform conditions, indicated by ρ_0 and $\mathrm{V}(\rho_0)$ respectively have been utilized. The steady state solution for homogeneous traffic flow is as follows:

$\rho_j(t) = \rho_0$

$V(\rho_j(t)) = V(\rho_0)$

Let$y_j(t)$ be a small perturbation to the steady-state density on site-j then

$\rho_j(t) = \rho_0 + y_j(t)$

$V(\rho_j(t)) = V(\rho_0(t)) + V'(\rho_0)y_j(t)$

Substituting $\rho_j(t) = \rho_0 + y_j(t)$ and put $y_j(t) = e^{ikj+zt}$ in into Eq. (7), then

$$e^{2z\tau} - e^{2z\tau} + \tau{\rho_0}^2(1+R)^2V'(\rho_0)e^{ik-1} \tag{8}$$

Now use $z = z_1(ik) - z_2(ik)^2$ in above equation and the compare the coefficient of (ik) And $(ik)^2$

Then we get the value of z_1 , z_2 and the value of $\tau = \frac{1}{a}$ where a is the driver sensitivity Linear analysis totally depend upon the value of " a ". Because the value of a and z_1 will use in to form the matlab code for linear analysis.

$$z_1 = -\rho_0{}^2(1+R)^2 V'(\rho_0) \quad (9)$$

$$z_2 = \frac{-3\tau z_1^2}{2} - \frac{\rho_0{}^2(1+R)^2 V'(\rho_0)}{2} \quad (10)$$

$$a = -3\rho_0{}^2(1+R)^2 V'(\rho_0) \quad (11)$$

$$\tau = \frac{1}{-3\rho_0{}^2(1+R)^2 V'(\rho_0)} \quad (12)$$

From Eq. (12), the parameter of road curvature actively help stabilize traffic flow, ensuring a steady flow profile that enhances driver comfort. Thus the stability condition hold for $\tau < \frac{1}{-3\rho_0{}^2(1+R)^2 V'(\rho_0)}$. the above stability criteria will become same as that of Nagatani [1] for R =0. The phase diagrams in density-sensitivity for the existing curved model and proposed model are compared in Fig.2. here R=0.5 and if we compare the value of curvature R=0.5 become when angle is π/4 . It is evident that the proposed model features a more stable zone for the given R = 0.5, which means an improvement over the current model. This underscores the significance of road curvature in ensuring a consistent and safe traffic flow. Figure 3 shows the neutral stability curves (solid curves) in density-sensitivity space and the apex of each curve indicates the critical point for different values of R. The stable region, free of traffic jams is above the neutral curves and the unstable region where density waves appear is below them. Figure 3 clearly illustrates that the amplitude of these curves grows with the increase in the values of R from 0.5 to 1.5 This suggests that higher values of R lead to the expansion of an unstable region. The neutral stability curves (solid curves) increase along with R, notice that the amount of traffic flow increases The dotted curves in Fig. 3Displays the neutral stability curves and coexisting curves (solid curves) that split the phase plane into three areas: the unstable area below the neutral stability curve, the metastable area between the coexisting curve and neutral stability curve, and the stable area above the coexisting curve.

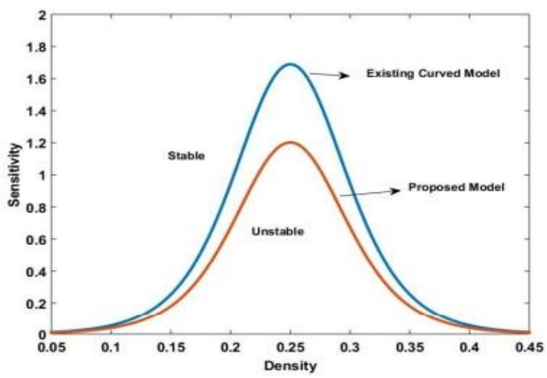

Figure 2: This phase diagram shows comparison between existing curved model and Proposed Model

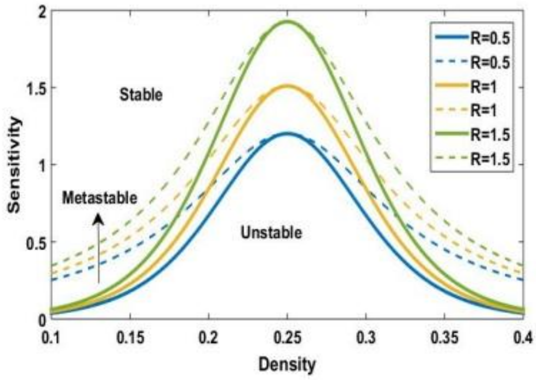

Figure 3: This phase diagram shows the impact of the curvature on the road

4. NONLINEAR ANALYSIS:

To investigate the nonlinear behavior near the critical point, we used the slower variables X and T. Nonlinear analysis allows for the examination of complex interactions between variables that may not be evident in a linear analysis. It can reveal emergent behaviors, stability, instability, and other intricate characteristics that are not apparent in simpler linear analysis. The analysis focused on a coarse scale, which means they looked at large-scale patterns in the traffic flow. For a small positive parameter ϵ, the slow variables X and T are defined as

$$X = \varepsilon(j + bt), T = \varepsilon^3 t \tag{13}$$

where b is constant to be determined. Let ρ_j satisfy the following equation:

$$\rho_j(t) = \rho_c + \varepsilon R(X, T) \tag{14}$$

The following nonlinear partial differential equation is obtained by using Eqs. (13) and (14) to expand Eq. (7), in the neighborhood of critical point, τ_c we define $\tau = \tau_c (1 + \epsilon^2)$ and choosing b= $-\rho_0{}^2(1+R)^2 V'(\rho_0)$.
we get

$$\boldsymbol{\epsilon^4}(\boldsymbol{\partial_T R} - \mu_1 \partial_X^3 R + \mu_2 \boldsymbol{\partial_X R^3}) + \boldsymbol{\epsilon^5}(\mu_3 \partial_X^2 R + \mu_4 \partial_X^4 R + \mu_5 \partial_X^2 \boldsymbol{R^3}) = 0 \tag{15}$$

where $V' = \frac{dv(\rho)}{d\rho}$ and $V''' = \frac{d^3 v(\rho)}{d\rho^3}$ at $\boldsymbol{\rho} = (\rho_c)$ Table 1 provides the coefficients μ_i (i = 1, 2, ..., 5) as follows:

Table 1: The coefficients μ_i of the model

Table 1:

The coefficients μ_i of the model	
μ_1	$-\frac{7}{6}b^2\tau^2 - \frac{\rho_0^2(1+R)^2}{6}$
μ_2	$\frac{\rho_c^2(1+R)^2 V'''(\rho_c)}{6}$
μ_3	$\frac{3}{2}b^2\tau$
μ_4	$\frac{15}{24}b^4\tau^3 + \frac{\rho_0^2(1+R)2}{24} + 3b\tau\mu_1$
μ_5	$\frac{\rho_0^2(1+R)^2 V'''(\rho_c)}{12} - 3b\tau\mu_2$

In order to derive the standard mKdV equation, we perform the following transformations in Eq. (15):

$$T' = \mu_1 T, R = \sqrt{\frac{\mu_1}{\mu_2}} R'$$

After implementing the transformation in Eq. (22), we obtain

$$\partial_T R' - \partial_X^3 R' + \partial_X R'^3 + \varepsilon \bar{M}[R'] = 0, \tag{16}$$

where $\bar{M}[R'] = \frac{1}{\mu_1}(\mu_3 \partial_X^2 R' + \frac{\mu_1 \mu_5}{\mu_2} \partial_X^2 R'^3 + \mu_4 \partial_X^4 R')$

We obtain the usual mKdV equation after neglecting the (ε) terms in Eq. (23) and intended kink-soliton solution is given by

$$R_0'(X, T') = \sqrt{c} \tanh \sqrt{\frac{c}{2}}(X - cT') \tag{17}$$

The solvability condition must be met in order to calculate the propagation velocity for the kink-antikink solution

$$(R_0' \bar{M}[R_0']) = \int_{-\infty}^{\infty} dX R_0' \bar{M}[R_0'] = 0, \tag{18}$$

with $\bar{M}[R_0'] = \bar{M}[R']$.

By solving Eq. (25), the value of c is

$$c = \frac{5\mu_2 \mu_5}{2\mu_2 \mu_4 - 3\mu_1 \mu_5}. \tag{19}$$

Hence, the "kink-antikink" solution is given by

$$\rho_j(t) = \rho_c + \varepsilon \sqrt{\frac{\mu_1 c}{\mu_2}} \tanh \sqrt{\frac{c}{2}}(X - c\mu_1 T), \tag{20}$$

with $\varepsilon^2 = \frac{\tau}{\tau_c} - 1$ and the amplitude A of the solution is

$$A = \sqrt{\frac{\mu_1}{\mu_2} \varepsilon^2 c}. \tag{21}$$

Two coexisting phases can be understood by the "kink-antikink" soliton solution. There is a congested high density phase as well as a low-density phase that is free to move, which may be separated from one another using the equation $\rho_j = \rho_c \pm A$ in the phase space (ρ, a).

5. NUMERICAL SIMULATION:

In this phage theoretical results have been given and the process is conducted for the new model incorporating periodic boundary conditions are as follows:

$$\rho_j(0) = \rho_j(1) = \begin{cases} \rho_0 - A & if\ 0 \le j < \frac{M}{2} \\ \rho_0 - A & if\ \frac{M}{2} \le j < M \end{cases}$$

In this context, σ denotes the initial disturbance, while M represents the total−number of sites, fixed at 100, with σ = 0.1, τ = 1/a Vmax = 2 and (ρ_0) = 0.25, respectively. In Figure 4, the two-dimensional distribution of density is depicted for different R values at a time step of 20, 300s. Figure. 4 displays the profiles of congestion traffic patterns with different coefficients of road curvature. According to the stability criterion, the amplitude of the density profile, illustrated in Figs. 4(a)-(b), steadily reduces with lower R values. Traffic flow becomes uniform at R = 0.5, as demonstrated in Fig. 4(c). We can see that although the vehicular system is unstable in patterns (a)–(b), the fluctuation of the traffic waves is significantly reduced as the effect coefficient R decreases. The above analysis reveals that the extent of the stability improvement is determined by the size of effect coefficient. Figure. 5 offer a clear depiction of the spatiotemporal evolution of density, specifically between time t = 20000 − 20300 correspond to the patterns in Fig. 4. In pattern (a) and pattern (b), a further decrease in R from 1.5 to 1 illustrates that the perturbation creates stop-and-go traffic that travels the other way. It's amplified with an decrease in the value of (a) and (b), which decreases the amplitude of these knik-antikink density waves. For the values

R = 0.5 and a = 1.2, a stable region is reached, the perturbation at the ending dies out over time, and the flow becomes uniform as shown in Fig. 5(c). The value of the curvature coefficient decreases, entered into the stable region and therefore the smooth traffic flow will be appear.

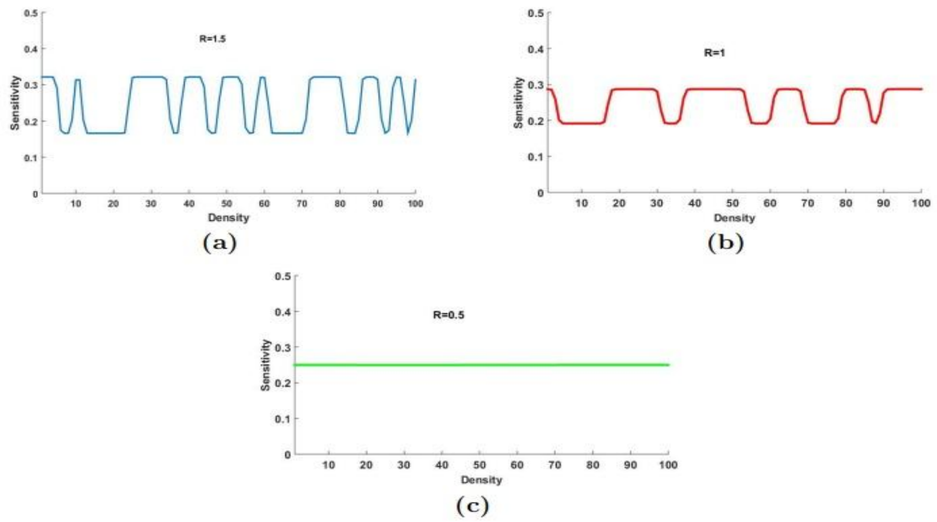

Figure 4: Density profiles at time t=20300s for $a = 1.2$ with different values of R

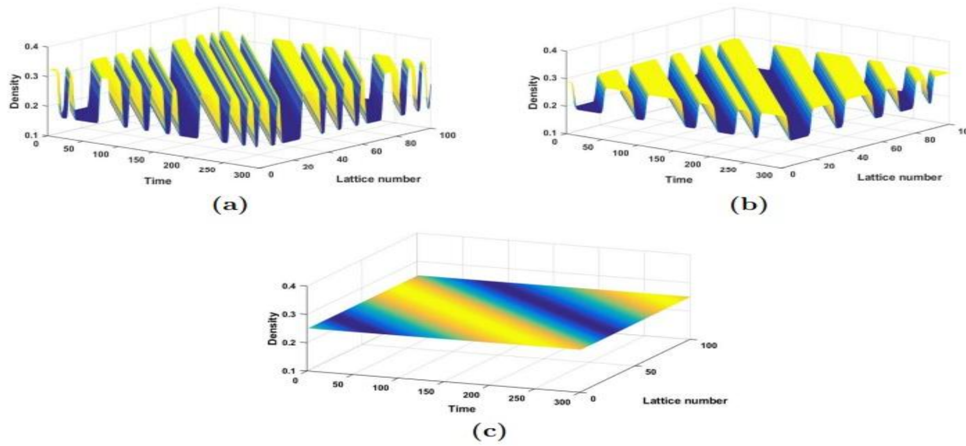

Figure 5: Spatiotemporal evolutions of density at time t=20300 for $a = 1.2$ with different values of R

6. CONCLUSION:

The present study introduces an innovative lattice hydrodynamic model that incorporates the influence of road curvature to better understand traffic flow behavior on curved roads. Traditional models often overlook geometric features such as curvature, which play a crucial role in real-world traffic flow. This approach provides a more accurate and realistic depiction of vehicle interactions, particularly in the case where road geometry can significantly affect driver behavior and spacing by explicitly integrating curvature into the modeling framework. A central aspect of this work is the derivation of a traffic flow stability condition using linear stability analysis. This analytical method enables the identification of the conditions under which small disturbances in vehicle spacing or speed either dissipate or grow over time, potentially leading to traffic instabilities. To delve deeper into the system's behavior near the onset of instability, a modified Korteweg–de Vries (mKdV) equation is derived using nonlinear perturbation techniques around the critical points on the neutral stability curve. This facilitates the investigation of complex wave-like patterns and nonlinear traffic phenomena, such as stop and-go waves, that emerge close to instability thresholds. Numerical simulations are conducted to explore the effects of varying curvature parameters on traffic flow behavior and to verify the theoretical results. These simulations reveal that, as road curvature increases—especially with sharper bends—traffic flow becomes less stable, and the likelihood of congestion significantly rises. The findings underscore the significant impact of road geometry on traffic stability and highlight the necessity of incorporating geometric design considerations into traffic flow modeling and infrastructure planning.

REFERENCE

[1] T. Nagatani, Modified kdv equation for jamming transition in the continuum models of traffic, Physica A: Statistical Mechanics and its Applications 261 (3-4) (1998) 599–607.

[2] X. Wang, J. Zhang, H. Li, Z. He, A mixed traffic car-following behavior model, Physica A: Statistical Mechanics and its Applications 632 (2023) 129299.

[3] Z. Wang, Y. Shi, W. Tong, Z. Gu, Q. Cheng, Car-following models for human-driven vehicles and autonomous vehicles: A Systematic Review, Journal of Transportation Engineering, Part A: Systems 149 (8) (2023) 04023075.

[4] X. Chen, M. Zhu, K. Chen, P. Wang, H. Lu, H. Zhong, X. Han, X. Wang, Y. Wang, Follownet: a comprehensive benchmark for car-following behavior modeling, Scientific Data 10 (1) (2023) 828.

[5] W. Du, Y. Li, J. Zhang, Stability control of a two-lane car-following model based on cluster synchronization of complex network, Optimal Control Applications and Methods (2023).

[6] X. Zhang, Z. Shi, J. Chen, et al., A bi-directional visual angle car-following model considering collision sensitivity, Physica A: Statistical Mechanics and its Applications 609 (2023) 128326.

[7] L. Yu, A new continuum traffic flow model with two delays, Physica A: Statistical Mechanics and its Applications 545 (2020) 123757.

[8] R. Mohan, G. Ramadurai, Heterogeneous traffic flow modelling using second-order macroscopic continuum model, Physics Letters A 381 (3) (2017) 115–123.

[9] A.K. Gupta, I. Dhiman, Analyses of a continuum traffic flow model for a nonlane-based system, International Journal of Modern Physics C 25 (10) (2014) 1450045.

[10] Y. Jiang, S. Wong, H. Ho, P. Zhang, R. Liu, A. Sumalee, A dynamic traffic assignment model for a continuum transportation system, Transportation Research Part B: Methodological 45 (2) (2011) 343–363.

[11] C. Wagner, C. Hoffmann, R. Sollacher, J. Wagenhuber, B. Sch¨urmann, Second-order continuum traffic flow model, Physical Review E 54 (5) (1996) 5073.

[12] H. Ge, R. Cheng, The "backward looking" effect in the lattice hydrodynamic model, Physica A: Statistical Mechanics and its Applications 387 (28) (2008) 6952–6958.

[13] G. Ma, K. Li, H. Sun, Modeling and simulation of traffic flow based on memory effect and driver characteristics, Chinese Journal of Physics 81 (2023) 144–154.

[14] J. Zhou, Z. Shi, W. Ke, P. Chao, Lattice hydrodynamic model for two-lane traffic flow on curved road, Nonlinear Dynamics 85 (2016) 1423–1443.

[15] Y. Jin, Z. Dan, S. Jie, K. Zhong, H. Zhang, W. Liang, P. Chao, Lattice hydrodynamic model for traffic flow on curved road with passing, Nonlinear Dynamics 89 (2017) 107–124.

[16] Q. Wang, R. Cheng, H. Ge, A novel lattice hydrodynamic model accounting for driver's memory effect and the difference of optimal velocity on curved road, Physica A: Statistical Mechanics and its Applications 559 (2020) 125023.

[17] D. Kaur, S. Sharma, A. K. Gupta, Analyses of lattice hydrodynamic area occupancy model for heterogeneous disorder traffic, Physica A: Statistical Mechanics and its Applications 607 (2022) 128184.

[18] J. Cao, S. Liang, K. Zhon, A novel lattice traffic flow model on a curved road, International Journal of Modern Physics C 26 (11) (2015) 1550121.

[19] T. Wang, R. Cheng, H. Ge, An extended two-lane lattice hydrodynamic model for traffic flow on curved road with passing, Physica A: Statistical Mechanics and its Applications 533 (2019) 121915.

[20] Q. Wang, R. Cheng, H. Ge, A new two-lane lattice hydrodynamic model on a curved road accounting for the empirical lane-changing rate, Engineering Computations 38 (4) (2021) 1532–1553.

[21] M. Bando, K. Hasebe, A. Nakayama, A. Shibata, Y. Sugiyama, Dynamical model of traffic congestion and numerical simulation, Physical Review E 51 (2) (1995) 1035.

[22] R Mehra, M Mehra, V K Sharma. "Investigating The Influence Of Driver Misconceptions On Road Behaviour Using A Novel Lattice Hydrodynamic Model" Educational Administration: Theory and Practice, vol. 30, no. 4, Apr. 2024, pp. 7804-12,